Effect of the Hydrolyzed Wheat Gluten/Wheat Starch Ratio on the Viscoelastic Properties of Rubber Composites

Lei Jong

National Center for Agricultural Utilization Research, Department of Agriculture, 1815 North University Street, Peoria, Illinois 61604

Received 14 October 2008; accepted 22 April 2009
DOI 10.1002/app.30653
Published online 2 July 2009 in Wiley InterScience (www.interscience.wiley.com).

ABSTRACT: Hydrolyzed wheat gluten (WG) and wheat starch (WS) showed substantial reinforcement effects in rubber composites. Because of the different abilities of WG and WS to increase the modulus of rubber composites, the composite properties could be adjusted by the variation of the ratio of WG to WS as a cofiller. WS and WG composites were less temperature-dependent than carbon black (CB) composites, and the cofiller composites became more temperature-dependent as the WG content increased. WS showed the greatest reinforcement effect, whereas WG and CB had similar effects. The cofiller composites had a reinforcement effect between those of the WG and WS single-filler composites. For fatigue and recovery properties, the initial structures of the WS composites were more stable at smaller strains, but they broke down at larger strains without much recovery. The WG and CB composites, on the other hand, had a less stable composite structure at smaller strains but had better recoverability. The cofiller composites reflected the characteristics of the single-filler composites. With respect to the residual structures of these composites after the strain cycles, the WG composites were the most elastic in the small strain region, and the structures of the cofiller composites became less elastic as the WS content increased. The extent of stress softening indicated that the WS composites had significant structural deformation and were less elastic in comparison with the WG and CB composites. The hydrolyzed WG-dominated composites exhibited viscoelastic behavior similar to that of CB composites. J Appl Polym Sci 114: 2280–2290, 2009

Key words: biomaterials; composites; reinforcement; rubber; viscoelastic properties

INTRODUCTION

To achieve the sustainability of the materials we use today, using sources other than petroleum or natural gas is required. Among the alternative sources are renewable agricultural materials. Agricultural materials are usually multicomponent and are complex mixtures of proteins, carbohydrates, fat, and ash. Because of their complex nature, a substantial number of studies are required to map their working principles. In this study, agricultural materials were investigated as reinforcement fillers in rubber composites. For practical applications (tires, seals, dampers, etc.), carbon black (CB) derived from petroleum or natural gas is the dominant filler used to reinforce crosslinked rubber materials. Some renewable materials such as dry soy protein and carbohydrates are rigid and can be used as rubber reinforcements. Soy products, including soy protein isolate,[1] defatted soy flour,[2] soy protein concentrate,[3] and soy spent flakes,[4] have been incorporated into rubber latex to form composites showing substantial reinforcement effects as measured by rheological and mechanical methods. Different reinforcement effects have been obtained from these soy products, which have different protein/carbohydrate ratios.[2,3] In this study, wheat gluten (WG) and wheat starch (WS) were mixed in different ratios as a cofiller, and their effects on the viscoelastic properties of rubber composites were investigated. To simplify the studies, the polymer matrix used in this study was a styrene–butadiene (SB) latex with a small amount of carboxylic acid containing monomer units. The carboxylated SB forms a crosslinked polymer matrix by the aggregation of ionic functional groups[5] without the complication of covalent reactions. In practical applications, conventional rubber formulations, including different types of rubber latices, crosslinking agents, coupling agents, and plasticizers, may also be used. To facilitate the understanding of this study, it should be mentioned that the major physical properties investigated were the dynamic modulus and recovery behavior. In our dynamic

Names are necessary to factually report on available data; however, the U.S. Department of Agriculture neither guarantees nor warrants the standard of the product, and the use of the name by the U.S. Department of Agriculture implies no approval of the product to the exclusion of others that may also be suitable.

Correspondence to: L. Jong (lei.jong@ars.usda.gov).

Journal of Applied Polymer Science, Vol. 114, 2280–2290 (2009)

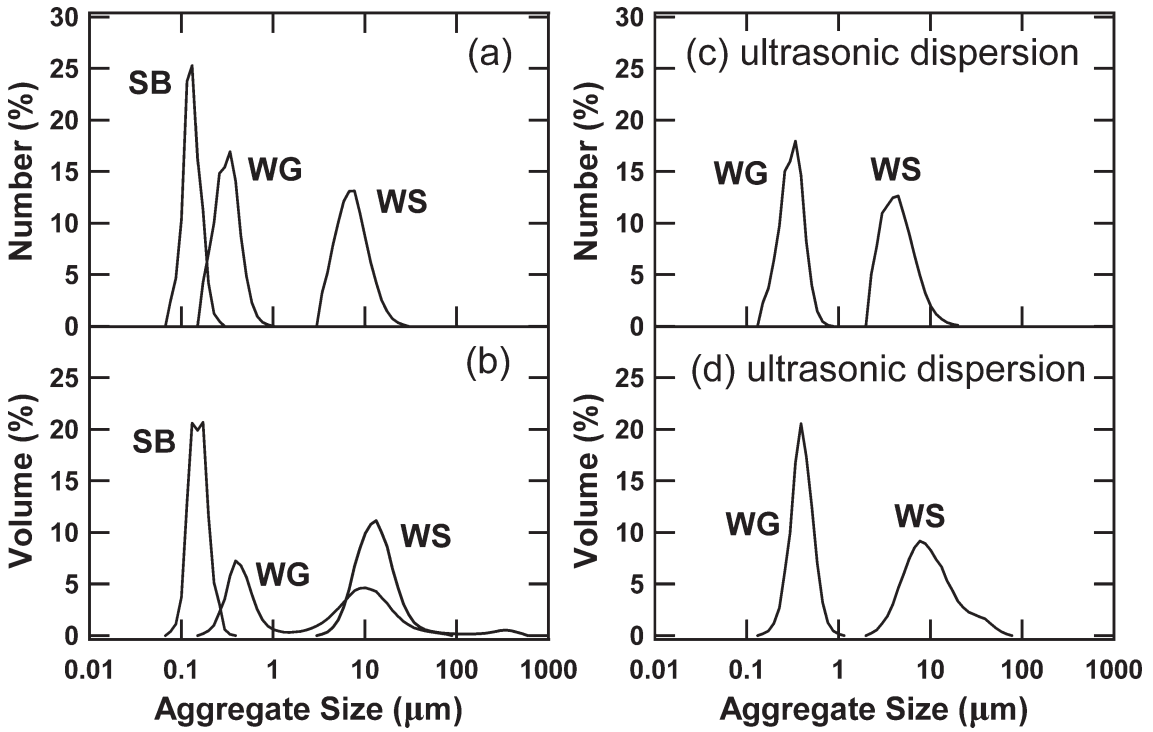

Figure 1 (a) Number-average aggregate size, (b) volume-average aggregate size, (c) number-average size after ultrasonic dispersion, and (d) volume-average size after ultrasonic dispersion.

experiments, material strength was defined by the dynamic modulus (yield strength). Elasticity was defined in our recovery experiments as the extent to which the materials recovered their original modulus.

EXPERIMENTAL

Materials

WG and purified WS were obtained from Sigma–Aldrich (Milwaukee, WI) and used directly without further purification. Sodium hydroxide, used to adjust the pH, was American Chemical Society grade. The carboxylated SB latex was a random copolymer of styrene, butadiene, and a small amount of carboxylic acid containing monomers (Rovene 9410, Mallard Creek Polymers, Charlotte, NC). According to the manufacturer's specifications, the glass-transition temperature and the styrene/butadiene ratio of the latex were −56°C and 25/75, respectively. The dried latex was not known to be soluble in any solvent or combination of solvents. The latex as received had approximately 50.5% solids and a pH of approximately 8.6. The volume-weighted mean particle size of the latex was approximately 150 nm.

Preparation of the WG and WS dispersions

WG is not water-soluble or dispersible because of its hydrophobic nature. To prepare WG and WS dispersions, an alkali hydrolysis reaction was carried out in a closed resin kettle equipped with a water condenser and a mixer. The WG, WS, or their mixtures were first homogenized in water at a pH of approximately 10.4 with an approximately 5.6% concentration for 15 min at 10^4 rpm. The dispersion was then cooked in the resin kettle by the temperature being raised from the ambient temperature to 95°C and kept there for 1 h with constant stirring. After the alkali hydrolysis reaction, the cooled dispersions were homogenized at 10^4 rpm for 1 h, and their pH was adjusted to 9 with sodium hydroxide. The resulting dispersions were observed to be stable under the ambient conditions for several days without precipitation. The mean aggregate size and distribution of these dispersions were measured with a Horiba (Horiba Instruments, Irvine, CA) LA-930 laser scattering particle size analyzer with a red-light wavelength of 632.8 nm and a blue-light wavelength of 405 nm. The instrument had a measurement range of 0.02–2000 μm. As shown in Figure 1, swollen WG aggregates in an aqueous dispersion had a number-average size of approximately 0.3 and a volume-average size of approximately 7 μm. The particle size of the SB latex is also included for comparison. Swollen WS aggregates in an aqueous dispersion had a number-average size of approximately 7 and a volume-average size of approximately 24 μm. The larger aggregates shown in the volume-average size distribution curves in Figure 1 were not permanent

aggregates but could be broken down by ultrasonic disruption, as shown in Figure 1(c,d). After 30 min of ultrasonic dispersion, swollen WG aggregates showed a uniform size distribution with a number-average size of approximately 300 and a volume-average size of approximately 380 nm. However, for practical purposes, all composite samples prepared in this study did not undergo ultrasonic treatment.

To compare the rubber properties of composites reinforced with WG, WS, and their mixtures with those of CB, an aqueous dispersion of CB N-339 (Sid Richardson Carbon Co., Fort Worth, TX) was prepared by the dispersion of approximately 100 g of CB in water with the aid of a surfactant, sodium lignosulfonate (Vanisperse CB, Lignotech USA, Rothschild, WI). The weight fraction of the surfactant based on CB was 3%. The dispersion was homogenized at 1.2×10^4 rpm for 1 h. The resulting CB dispersion had a solid content of 11.5%. The number-average size and volume-average size of the CB aggregates were measured to be 280 and 540 nm, respectively.

Preparation of the elastomer composites

The dispersions of WG, WS, or their mixtures were first adjusted to a desired pH value, and SB latex that had already been adjusted to the same pH was then added to the aqueous dispersion and mixed homogeneously to form composites with four different filler concentrations (10, 20, 30, and 40 wt %). The homogeneous composite mixtures were then quickly frozen in a rotating shell freezer at about −40°C, and this was followed by freeze drying in a freeze dryer (Labconco, Kansas City, MO). The composites of CB were also prepared with the same procedure. The moisture content of the dried composite crumb was less than 2%. The freeze-dried crumb was then compression-molded in a window-type mold at 138 MPa and 110°C for 2.5 h. After compression molding, the samples were relaxed and further annealed at 90 and 140°C for 24 h at each temperature. The annealing was used to dry the samples because moisture behaves as a plasticizer for WG and WS and affects the composite moduli. The torsion bar of carboxylated SB rubber was also prepared with the same process used for the other composites, but the torsional bars of 100% WG and WS were prepared with a plunge-type mold and were compressed at 140°C and 172 MPa. The dried samples had a moisture content less than 0.8% as measured by a halogen moisture analyzer (HR73, Mettler-Toledo, Columbus, OH) at 105°C for 60 min. The densities of the samples were measured with a density bottle (Gay-Lussac bottles) with a low-viscosity poly(dimethylsiloxane) as the immersion liquid. The measured densities of SB, WG, WS, and CB were 1.00, 1.34, 1.54, and 1.73 g/cm^3, respectively. The uncertainty in the density measurement was less than 1%. The composite density could be estimated from the component densities under the assumption that their volumes were additive. The difference between the calculation and the measurement in such estimation was less than 2%. For lightweight applications, agricultural fillers have an advantage over CB or inorganic fillers at the same volume fraction for some applications.

Dynamic mechanical measurements

A Rheometric ARES-LSM rheometer (TA Instruments, Piscataway, NJ) with TA Orchestrator software (version 7.1.2.3) was used for the dynamic mechanical measurements. All data presented in this study were based on the measurements of one well-prepared sample. To study the thermal mechanical properties of the composites, temperature ramp experiments were conducted with torsion rectangular geometry at a heating rate of 1°C/min in the temperature range of −70 to 140°C. When torsion rectangular geometry was used, torsional bars with dimensions of approximately $50 \times 12.5 \times 6$ mm^3 were mounted between a pair of torsion rectangular fixtures, and the dynamic mechanical measurements were conducted at a frequency of 0.16 Hz (1 rad/s) and a strain of 0.05%. One well-prepared specimen was used for each composite measurement. The uncertainty of the modulus measurements mainly arose from the uncertainty in the measurement of the specimen dimensions. The dimensions of rigid specimens can be more accurately measured in comparison with those of softer specimens. The uncertainty was determined by the measurement of the most rigid composite, 40% WS/SB, and the softest composite, 10% CB/SB. The range of the standard deviation for the composite moduli was determined to be ±3% to ±10% by the measurement of triplicate specimens.

To study the stress-softening effect, strain sweep experiments were conducted with torsional rectangular geometry to measure the oscillatory storage modulus [$G'(\omega)$] and oscillatory loss modulus [$G''(\omega)$]. The shear-strain-controlled rheometer was capable of measuring the oscillatory strain down to 3×10^{-5} % strain. The rheometer was calibrated in terms of the torque, normal force, phase angle, and strain with the instrument's standard procedure. A rectangular sample with dimensions of approximately $25 \times 12.5 \times 6$ mm^3 was inserted between the top and bottom fixtures. The gap between the fixtures was approximately 7 mm to achieve a strain of approximately 14%. A sample length shorter than 5 mm was not desirable because of the resulting shape change from the clamping at both ends of the sample. The frequency used in the measurements was 1 Hz. $G'(\omega)$ and $G''(\omega)$ were measured over a

strain range of approximately 0.007–14%, which was incremented by 40 equally spaced data points per decade on a logarithmic scale. The residence time at each strain was automatically controlled by the instrument. The actual strain sweep range was limited by the sample geometry and motor compliance at a large strain and by the transducer sensitivity at a small strain. The data out of the transducer range were rejected. Although harmonics in the displacement signal may be expected in a nonlinear material, a previous study[6] indicated that the harmonics are not significant if the shearing does not exceed 100%. Each sample was conditioned at 140°C for 30 min to reach an equilibrated dimension and then subjected to eight cycles of dynamic strain sweeping to study the stress-softening effect. The delay between strain cycles was 100 s. For clarity, only data from the first, fourth, and eighth cycles are presented in the figures. To measure the recovery behaviors at 140°C, the original storage modulus (G'_0) of the samples was first measured at 0.05% strain and 0.16 Hz (1 rad/s). Then, the samples were subjected to a large strain of 10% for 30 s, and this was followed by periodic measurements of the storage modulus (G') at a 0.05% strain and 0.16 Hz (1 rad/s) to record the recovered modulus.

RESULTS AND DISCUSSION

Temperature-dependent modulus

The temperature-dependent modulus [G′(T)] is a useful property that yields information on how the modulus changes within a temperature range for a certain application. Figure 2 shows $G'(T)$ of WG, WS, and CB at four filler concentrations (10, 20, 30, and 40%). Even though these composites were different materials, they showed temperature-dependent features similar to those of the SB polymer. As the temperature increased, their moduli showed an initial drop due to the glass transition of the SB polymer, and this was followed by a secondary transition and a rubber plateau region. The primary glass-transition temperature of the SB matrix at about −50°C was assigned by comparison to noncarboxylated SB with a similar styrene content.[7,8] Because carboxylic acid groups are the only difference between SB and carboxylated SB, it is reasonable to assign the secondary transition at approximately 0°C to the ionic aggregation[9–11] of the SB matrix. One hundred percent WS and WG are also included in the upper portion of the figure for comparison; it shows that WG had greater temperature dependence than WS. The temperature-dependent G' values of the cofiller composites are shown in Figure 3, and their curve features are similar to those in Figure 2. To determine the difference between these data curves, a G′(0°C)/G′(140°C) ratio was taken for each composite and is shown in Figure 4; 0–140°C represents a typical application temperature range for the composites. The ratio indicates the tendency of the modulus to vary with temperature in each composite. The comparison of different composites in Figure 4 shows that WS was the least temperature-dependent and CB was the most temperature-dependent. Among the cofiller composites, the composites with a greater amount of WG were affected more by temperature changes, and this was consistent with the temperature-dependent behavior of 100% WG and WS in Figure 2. Overall, the moduli of the WG- and WS-reinforced composites appeared to be less affected by temperature changes than the moduli of the CB composites. When the lower limit of the temperature

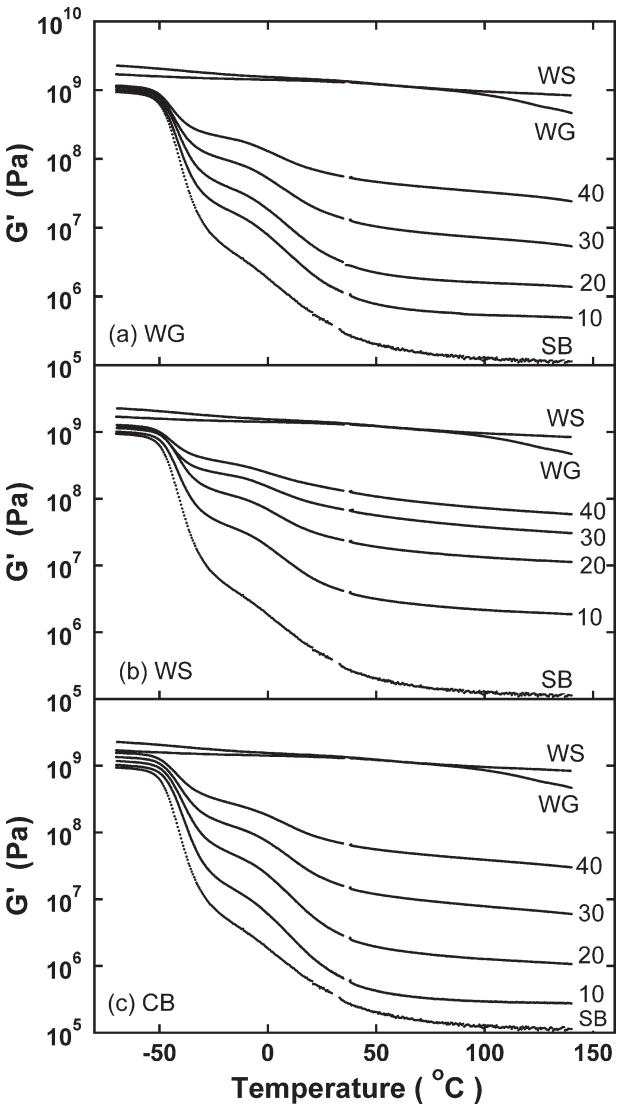

Figure 2 Elastic moduli of single-filler composites with different filler concentrations in the temperature range −70 to 140°C. The weight fraction and filler type of the single-filler composites are shown near their curves.

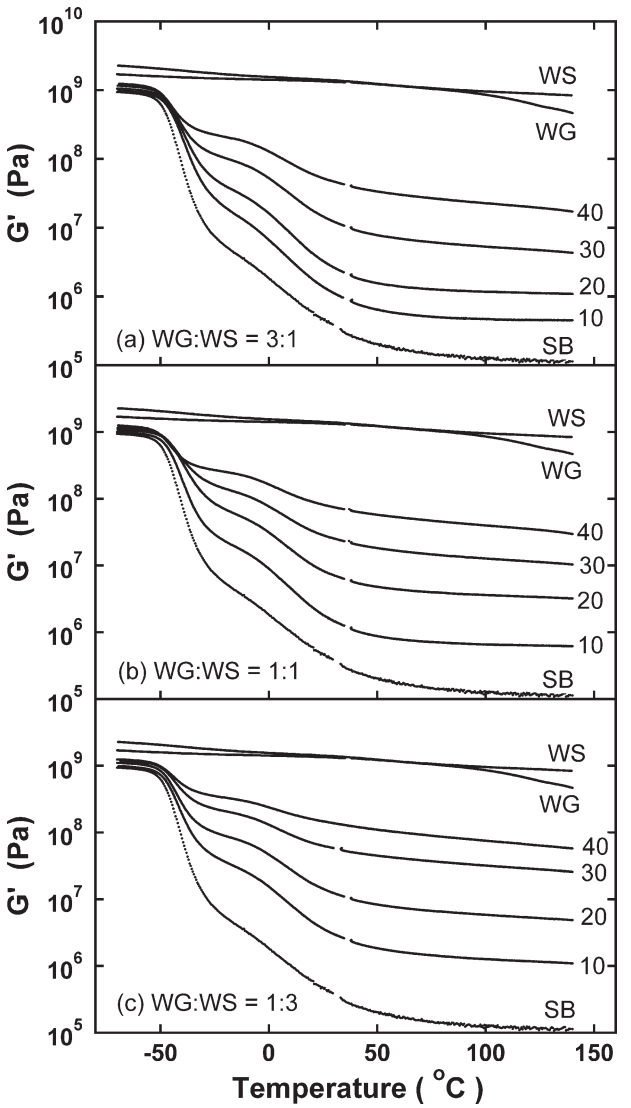

Figure 3 Elastic moduli of WG/WS cofiller composites with different cofiller ratios and different filler concentrations in the temperature range −70 to 140°C. The weight fraction of the cofiller is shown at the end of each curve. The cofiller ratios are also shown on the graphs.

range was extended to −20°C, the G' ratios of −20 to 140°C still yielded the same trend shown in Figure 4.

To compare the plateau moduli of different composites, the elastic moduli at 140°C were plotted in Figure 5, which shows that WS-reinforced composites had the greatest moduli and that the moduli of cofiller composites decreased with an increase in the WG content. Among these composites, similar modulus curves were observed for WG, CB, and 3 : 1 WG/WS composites. This may indicate that the WG and 3 : 1 WG/WS composites prepared in this study have potential to be CB substitutes for some rubber applications. Moreover, practical applications are based on the filler weight fraction, not the volume fraction. Nonetheless, the relationship between the modulus and volume fractions is also provided in Figure 5(b) for comparison. As for the reinforcement effect expressed as the modulus increase with respect to the SB polymer, the ratios are listed in Table I. WS showed the largest reinforcement effect, whereas the 3 : 1 WG/WS composite displayed the smallest reinforcement effect.

Fatigue and recovery behavior

The fatigue properties of these composites provide an understanding of the resilience of the materials, and we investigated them by stressing the composites with consecutive dynamic strain cycles; the effects are shown in Figures 6 and 7 for the single-filler and cofiller composites, respectively. To understand these apparently similar strain data, three characteristics were analyzed: (1) the effect of the strain cycle on G' retention, (2) the shifting of the G'' maximum (G''_{max}) along the strain axis, and (3) the height reduction of G''_{max}.

The retention of G' in the small strain region after the eight cycles of strain deformation was used to characterize the fast recovery behavior during the experiment. These data, shown graphically in Figures 6 and 7, are listed in Table II, which shows that 20% composites retained more of the original modulus than 30% composites as expected. WS composites were the least elastic in comparison with WG or CB composites, the elasticity of the cofiller composites increased as the WG content was increased, and the modulus retention of WG composites was comparable to that of CB composites.

For the loss modulus (G'') under consecutive strain cycles, the energy dissipation processes of the

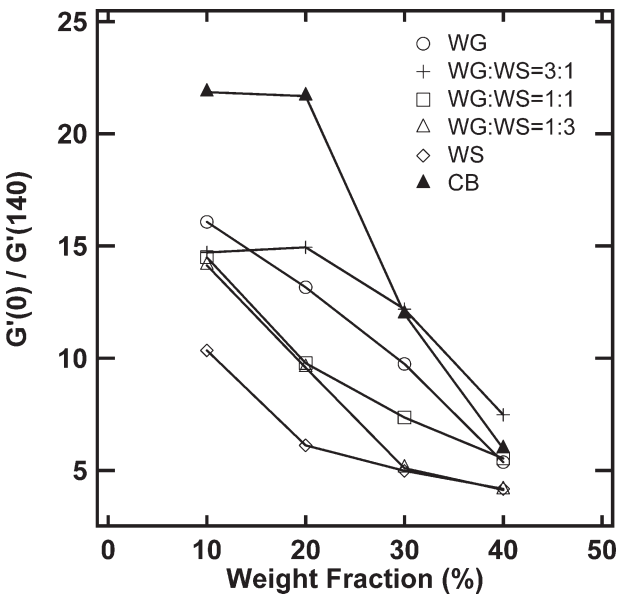

Figure 4 Ratio of G' at 0°C [$G'(0)$] to G' at 140°C [$G'(140)$] for both single-filler and cofiller composites plotted against the filler concentrations.

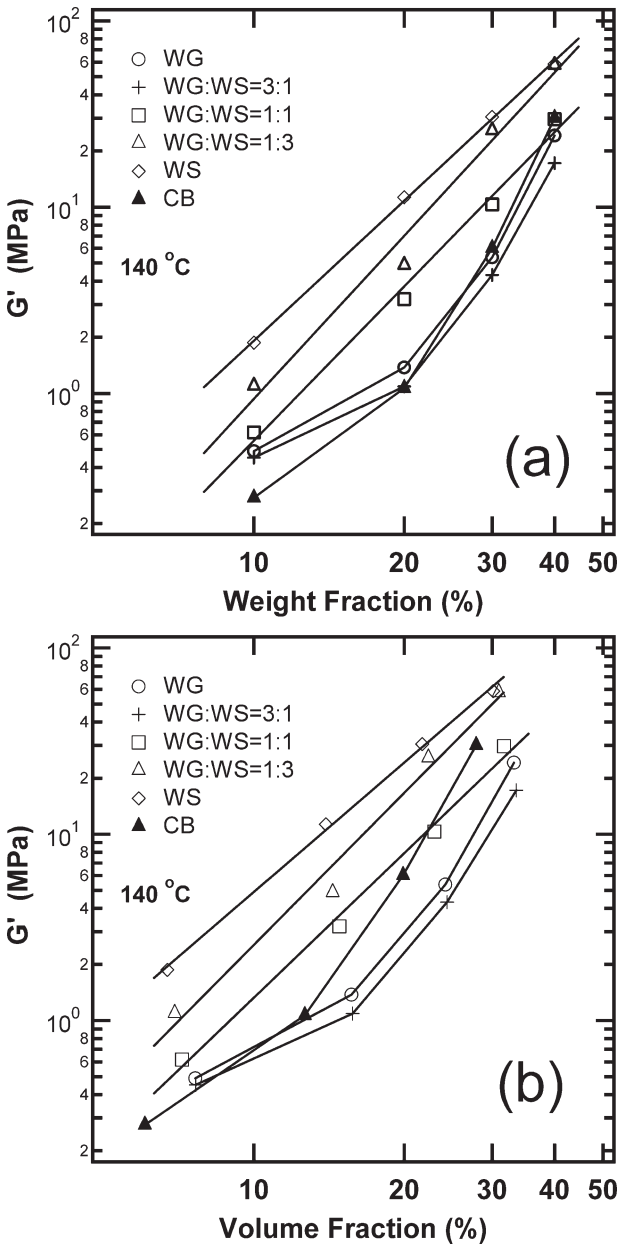

Figure 5 Elastic moduli of both single-filler and cofiller composites with different filler concentrations at 140°C: (a) weight fraction and (b) volume fraction.

composites (Figs. 6 and 7) became less pronounced, and their maxima were shifted from a larger strain to a smaller strain, as shown in Table III. The structure responsible for the energy dissipation process was obviously reduced after the eight strain cycles. A loss maximum of a composite that occurs at a larger strain percentage indicates a more resilient structure; this means that a greater extent of deformation is required to break down the filler-related network structure. The filler-related network structure is defined here as a network formed through the connectivity of fillers and immobilized polymer chains. In such a description, the effect of interfaces from filler–filler and filler–polymer interactions is already incorporated and contributes to the modulus of the filler-related network structure. With respect to the analysis given in Table III, it should also be mentioned that the concept of this analysis is qualitative, and only the trends are extracted from the data. The data show that G''_{max} occurred at a larger strain for 20% composites versus 30% composites, indicating that their filler-related network structure was more elastic. This also indicates that WS composites were stronger in the smaller strain region in comparison with WG and CB composites, but they were unable to recover once they were broken down by the dynamic strain cycles. The trend, however, is not as clear in the cofiller composites as that in the single-filler composites, and this suggests that the cofiller composites may have a more complex filler-related network structure.

A greater reduction in the magnitude of G''_{max} values by the strain cycles indicates a greater extent of breakdown in the original filler network structures. It is postulated here that the height reduction of G''_{max} is a net effect of structure breakdown and recovery. Table III shows that WS composites had a greater reduction in G''_{max} than WG and CB composites, and this indicates that the WS-related network structure was more brittle and more structures were broken down by a larger strain without much recovery. In cofiller composites, the composites with a greater amount of WS appeared to have an increasing extent of structure breakdown with the strain cycles.

To examine the recovery behavior for these composites more closely, the composites were subjected to a deformation stimulus and allowed to recover from it. As shown in Figure 8, WG composites showed the best recovery behavior among the 30% filled composites and were comparable to CB composites. Both 20% WG and CB composites showed a recovered modulus that was greater than the original modulus ($G'/G'_0 > 1$); this indicated a structural rearrangement resulting from the application of 10% strain. For cofiller composites, the ability to recover the original modulus was reduced by the increasing

TABLE I
Increase in the Composite Modulus Versus SB

Filler fraction (%)	10	20	30	40
Single filler				
WG	4	12	47	213
WS	17	100	269	518
CB	2	9	53	265
Cofiller				
3 : 1 WG/WS	4	10	38	152
1 : 1 WG/WS	6	28	91	262
1 : 3 WG/WS	10	43	227	509

The increase in the modulus is defined as G'(Composite)/G'(SB) at 140°C.

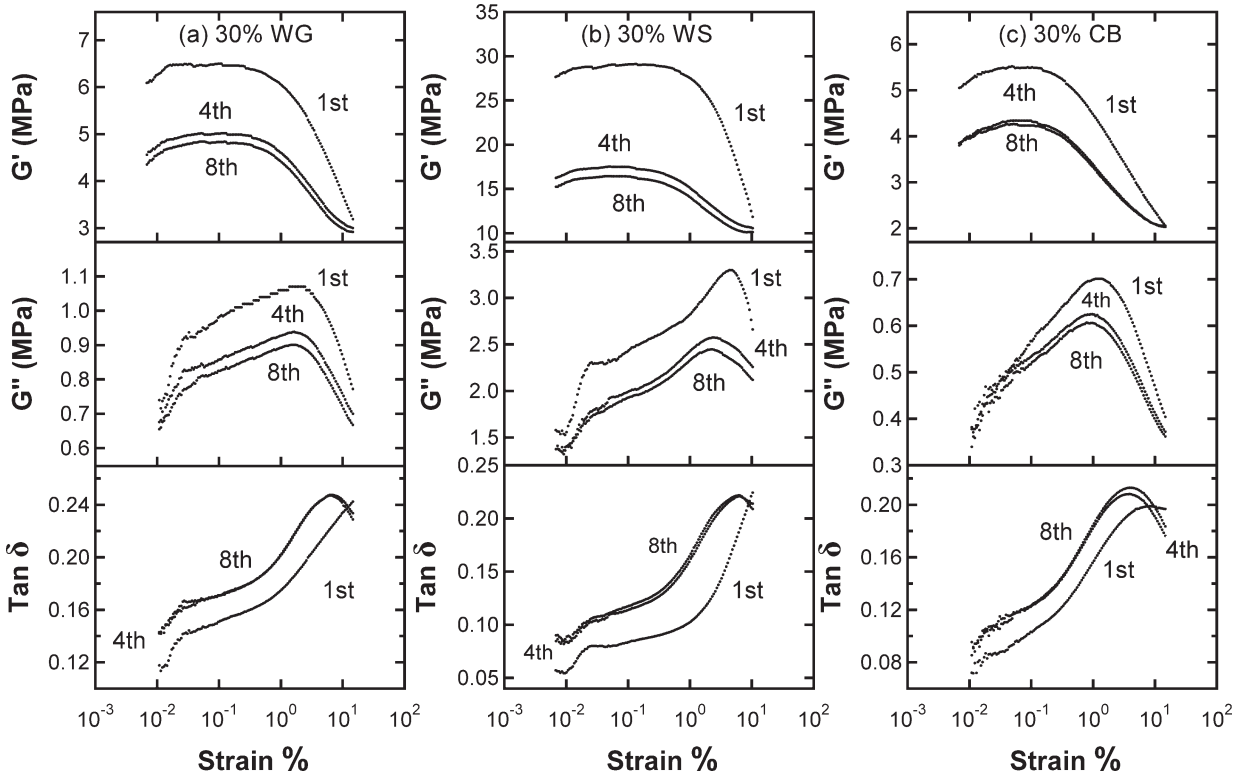

Figure 6 Strain sweep experiments of composites reinforced with 30 wt % WG, WS, or CB at 140°C. For clarity, only the first, fourth, and eighth strain cycles are shown.

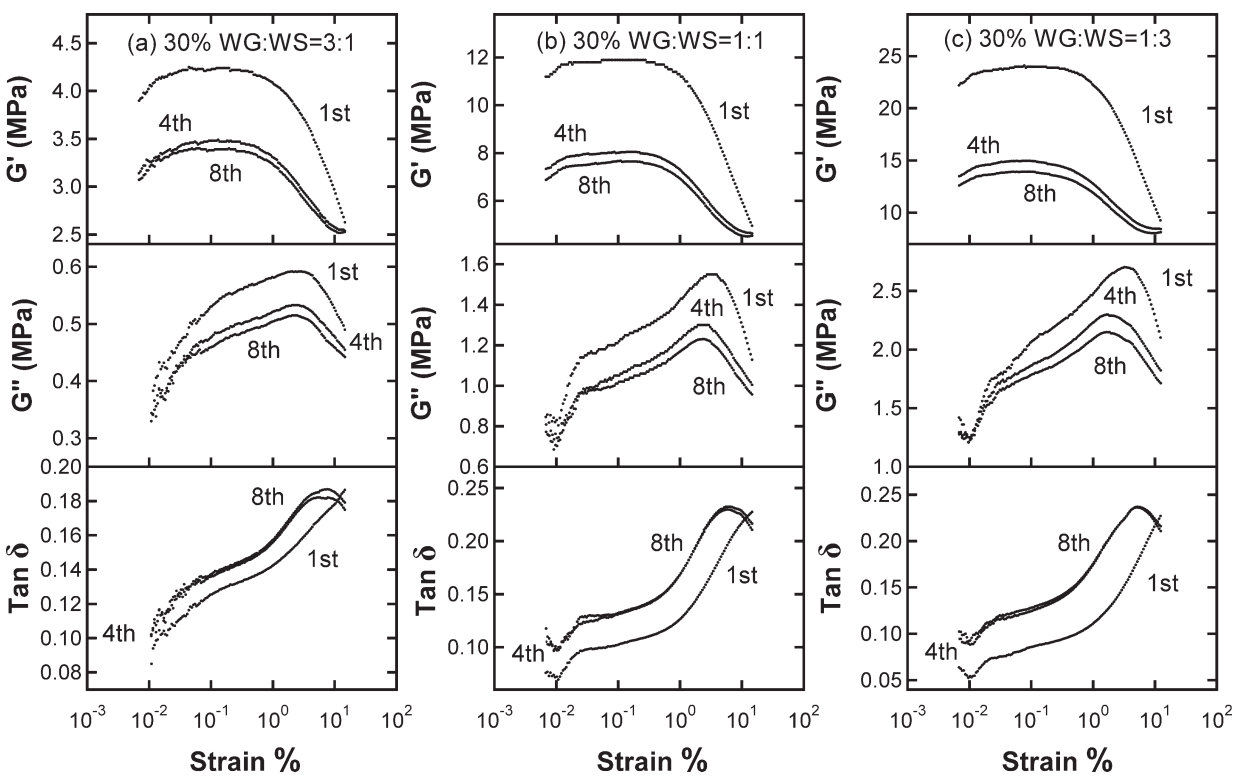

Figure 7 Strain sweep experiments of composites reinforced with 30 wt % cofiller at 140°C. The cofiller ratios are indicated in the graphs. For clarity, only the first, fourth, and eighth strain cycles are shown.

TABLE II
Retention of G' After Eight Strain Cycles

Filler fraction (%)	20	30
Single filler		
WG	90%	75%
WS	69%	57%
CB	94%	77%
Cofiller		
3 : 1 WG/WS	94%	80%
1 : 1 WG/WS	89%	64%
1 : 3 WG/WS	69%	58%

The values are the ratio of G' of the eighth strain cycle to that of the first strain cycle at 0.05% strain.

amount of WS in the composites, and the recovery behavior also depended on the filler concentration. In general, better recovery behavior was observed at lower filler concentrations, and this suggested that more polymer chains incorporated into the filler-related network structure tended to produce better recovery behavior.

To summarize the observations in this section, it can be concluded that the WS filler-related network structure was stronger and more resilient in the smaller strain region, but it was brittle in the larger strain region. WG and CB, on the other hand, had a filler-related network structure that was easier to break up in the smaller strain region, but it had better recoverability. The cofiller composites reflected a combination of the characteristics of the single-filler composites.

Characteristics of the residual structure

The residual structure is defined as the reversible structure after composites are subjected to dynamic strain cycles and reach an equilibrium state. Because these strain curves are similar in their features, one way of comparing these curves is to fit the data to a mathematical model and to compare the fitting parameters. Historically, Payne[12–14] reported the reduction of the shear elastic modulus with increasing strain on CB-filled rubbers in the early 1960s. Later, Kraus[15] proposed a phenomenological model based on Payne's postulation of filler networking. The model is based on the aggregation and deaggregation of CB agglomerates. In this model, the CB contacts are continuously broken and reformed under a periodic sinusoidal strain. On the basis of this kinetic aggregate-forming and -breaking mechanism at equilibrium, the elastic modulus can be expressed as follows:

$$\frac{G'(\gamma) - G'_\infty}{G'_0 - G'_\infty} = \frac{1}{1 + (\gamma/\gamma_c)^{2m}} \quad (1)$$

where γ is the applied strain, G'_∞ is equal to $G'(\gamma)$ at a very large strain, G'_0 is equal to $G'(\gamma)$ at a very small strain, γ_c is a characteristic strain at which $G'_0 - G'_\infty$ is reduced to half of its zero-strain value, and m is a fitting parameter related to filler aggregate structures. Equation (1) has been shown to describe the behavior of $G'(\gamma)$ in CB-filled rubber reasonably well.[16] G'' and the loss tangent (tan δ), however, do not show good agreement with experiments,[17] likely because of the uncertainty in the formulation of a loss mechanism.

In this study, G' from the eighth strain cycle was used as an equilibrated composite modulus in the strain cycle experiments shown in Figure 9, and the

TABLE III
Reduction of G'' After Eight Strain Cycles

	30% filler		20% filler	
Composition	G''_{max} shift[a]	G''_{max} reduction (%)[b]	G''_{max} shift[a]	G''_{max} reduction (%)[b]
Single filler				
WG	1.8→1.6	16	4.0→3.2	7
WS	4.3→2.3	26	5.8→3.9	14
CB	1.23→0.78	14	1.8→1.5	4
Cofiller				
3 : 1 WG/WS	2.4→2.2	13	5.4→4.3	4
1 : 1 WG/WS	3.25→2.44	21	5.8→4.7	5
1 : 3 WG/WS	3.25→1.64	21	3.7→2.8	16

[a] Shifting of G''_{max} in terms of the strain percentage from the first strain cycle to the eighth strain cycle.
[b] Percentage reduction of G''_{max} of the eighth strain cycle versus that of the first strain cycle.

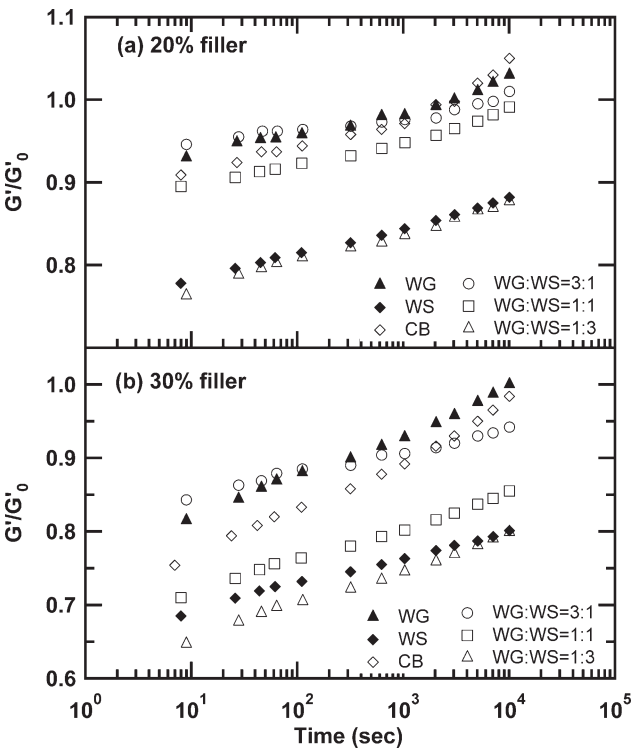

Figure 8 Modulus recovery of 20 and 30% filled composites measured at 140°C.

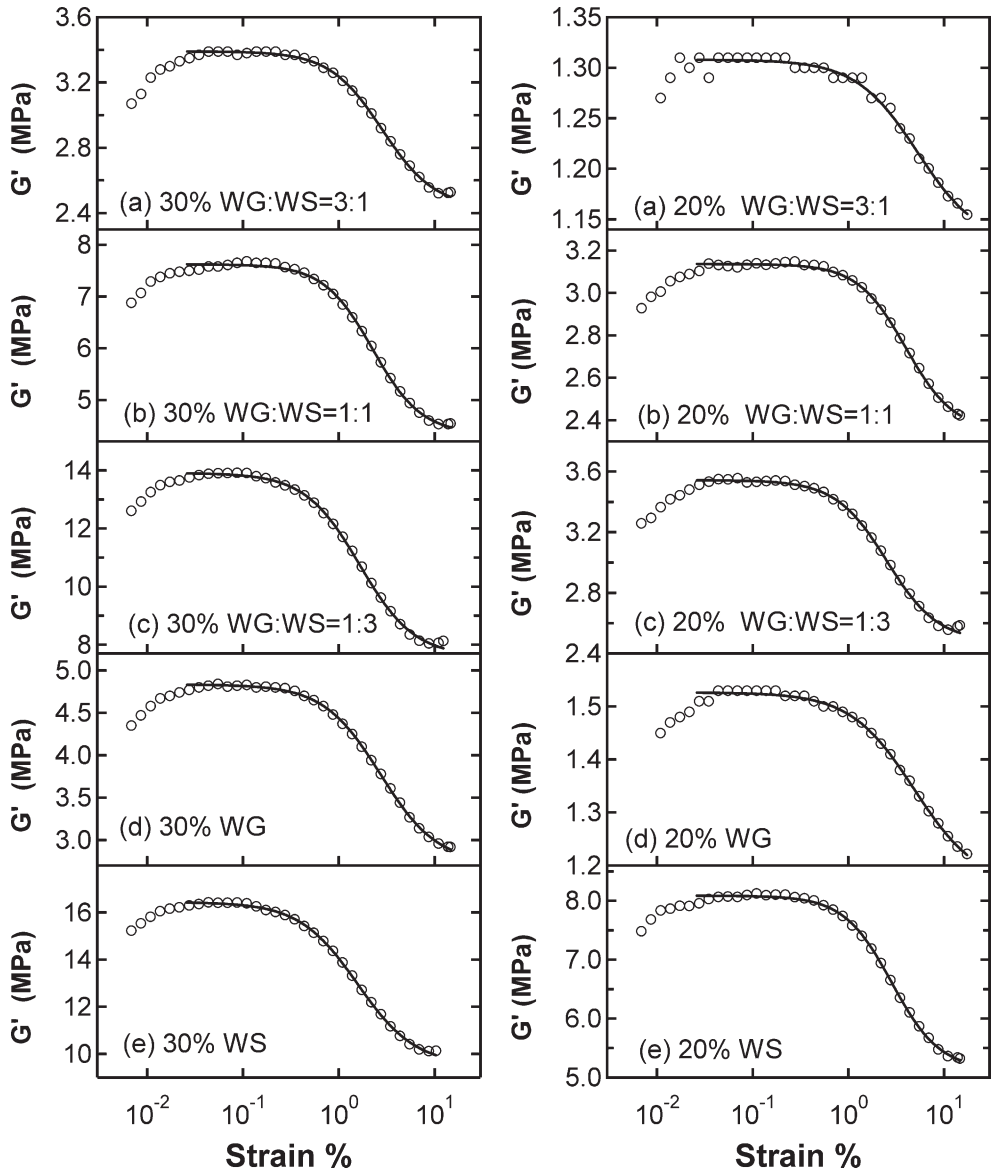

Figure 9 Composites with 30% filler. The eighth cycles of the strain sweep experiments at 140°C and 1 Hz are shown. For clarity, the number of data points, represented by circles, is reduced, and the solid lines are fitted from the Kraus model.

fitting parameters are summarized in Table IV. The model fit and standard deviation of the fit coefficients in Table IV were based on a 99.73% confidence level with Igor Pro 6.0 software. This model fitting analysis was performed to analyze the residual structures only after the initial structure had been broken down by the dynamic cycles. The discussion based on this analysis should not be confused with the discussion mentioned earlier on the fatigue and recovery properties, which were based on the change from initial structures to residual structures.

For the residual structures of these composites, a smaller m values indicates a continuous decrease in G' with increasing strain and suggests a smoother and continuous breakup of the filler network structure as the strain is increased. On the other hand, a larger m value indicates a structure that does not yield at lower strains but will start to break up when a certain strain is reached. When m values are similar between two composites, a smaller γ_c value is related to a composite that breaks up substantially at smaller strains.[2–4] γ_c, therefore, has a physical meaning associated with the brittleness of the composite structures. On the basis of Figure 9 and Table IV, the fitting using the Kraus model was generally acceptable, except when a significant G''_{max} value occurred in the small strain region, which gave rise to a greater uncertainty in m values. Theoretically, the model did not take into account the G'' transition

TABLE IV
Fitting Parameters of the Shear Elastic Modulus

Composition	Best fit m[a]	γ_c (%)	G'_0 (MPa)	G'_∞ (MPa)	$\Delta G'$ (MPa)[b]
30% single filler					
WG	0.73 ± 0.03	2.70 ± 0.10	4.83 ± 0.01	2.72 ± 0.04	2.11
WS	0.71 ± 0.03	1.56 ± 0.05	16.4 ± 0.04	9.51 ± 0.11	6.89
CB	0.62 ± 0.03	1.39 ± 0.06	4.30 ± 0.02	1.92 ± 0.05	2.38
30% cofiller					
3 : 1 WG/WS	0.79 ± 0.04	2.82 ± 0.13	3.39 ± 0.01	2.43 ± 0.02	0.96
1 : 1 WG/WS	0.85 ± 0.05	2.24 ± 0.09	7.62 ± 0.02	4.34 ± 0.07	3.28
1 : 3 WG/WS	0.76 ± 0.03	1.64 ± 0.06	13.91 ± 0.04	7.60 ± 0.11	6.31
20% single filler					
WG	0.65 ± 0.06	4.85 ± 0.59	1.53 ± 0.003	1.16 ± 0.02	0.37
WS	0.86 ± 0.04	2.83 ± 0.11	8.09 ± 0.02	5.13 ± 0.07	2.96
CB	0.65 ± 0.06	2.68 ± 0.25	1.03 ± 0.003	0.73 ± 0.01	0.30
20% cofiller					
3 : 1 WG/WS	0.67 ± 0.09	5.28 ± 0.96	1.31 ± 0.002	1.12 ± 0.02	0.16
1 : 1 WG/WS	0.86 ± 0.05	3.97 ± 0.22	3.14 ± 0.01	2.35 ± 0.03	0.79
1 : 3 WG/WS	0.81 ± 0.04	2.52 ± 0.10	3.54 ± 0.01	2.48 ± 0.02	1.06

The data are from the eighth strain cycle measured at 140°C.
[a] Best fit of the shear elastic modulus versus strain with the Kraus model.
[b] $\Delta G' = G'_0 - G'_\infty$.

in the very small strain region ($<\sim$ 0.02% strain), which can be clearly seen in Figure 6(a,b) and in Figure 7(b,c). Therefore, we chose to start the fitting range from 0.025% strain without taking into account the initial curvature of the strain curves shown in Figure 9.

The m values of all composites listed in Table IV are in the range of 0.6–0.9 and are not significantly different between 20% and 30% filled composites. Comparing 20% and 30% filled composites, we found that the γ_c values increased as more polymers were incorporated into the filler network structure. Moreover, the γ_c values decreased in the order of WG > WS > CB, indicating that the residual structures of WG composites were the most elastic in the small strain region. For the cofiller composites, the γ_c values decreased as the WS content increased, reflecting the γ_c values of the WG and WS composites. To compare the extent of stress softening between different composites, the modulus difference ($\Delta G' = G'_0 - G'_\infty$) was calculated for each composite and is listed in the last column of Table IV. The $\Delta G'$ values were similar for the WG and CB composites but were larger for the WS composites, indicating that the WS composites had experienced a significant structural change and were less elastic than the WG and CB composites.

CONCLUSIONS

This study shows that hydrolyzed WG and WS have substantial reinforcement effects in rubber composites. The significant difference between the abilities of WG and WS to increase the modulus of rubber composites provides a way to adjust composite properties by the variation of the ratio of WG to WS as a cofiller. The temperature-dependent moduli indicated that WS and WG composites were less temperature-dependent than CB composites, and the temperature dependence of the cofiller composites increased with the WG content increasing. Compared to the SB polymer, WS had the greatest reinforcement effect, whereas WG and CB had similar effects. The cofiller composites showed a reinforcement effect between those of WG and WS single-filler composites.

For fatigue and recovery properties, the initial WS filler-related network structure was stronger and resilient in the smaller strain region, but it broke down significantly in the larger strain region without much recovery. The composite structures of WG and CB, on the other hand, broke up easily in the smaller strain region but had better recoverability. The cofiller composites reflected a mixture of the characteristics exhibited by the single-filler composites.

With respect to the residual structures of these composites, WG composites were the most elastic in a small strain region. For the cofiller composites, the γ_c values suggested that the composite structures became easier to break up as the WS content increased, reflecting the γ_c values of WG and WS composites. As for $\Delta G'$ values, they were similar between WG and CB composites but were larger for WS composites, indicating that WS composites had significant structural deformation and were less elastic in comparison with WG and CB composites. This study indicates that hydrolyzed WG and hydrolyzed

WG-dominated composites exhibit viscoelastic properties similar to those of CB composites.

References

1. Jong, L. J Polym Sci Part B: Polym Phys 2005, 43, 3503.
2. Jong, L. J Appl Polym Sci 2005, 98, 353.
3. Jong, L. Compos A 2006, 37, 438.
4. Jong, L. Compos A 2007, 38, 252.
5. Kan, C. S.; Blackson, J. H. Macromolecules 1996, 29, 6853.
6. Chazeau, L.; Brown, J. D.; Yanyo, L. C.; Sternstein, S. S. Polym Compos 2000, 21, 202.
7. Furuta, I.; Kimura, S.-I.; Iwama, M. In Polymer Handbook, 4th ed.; Brandrup, J.; Immergut, E. H.; Grulke, E. A., Eds.; Wiley: New York, 1999; p V/3.
8. Loadman, M. J. R. J Therm Anal 1986, 31, 1183.
9. Richard, J. Polymer 1992, 33, 562.
10. Zosel, A.; Ley, G. Macromolecules 1993, 26, 2222.
11. Kan, C. S.; Blackson, J. H. Macromolecules 1996, 29, 6853.
12. Payne, A. R. J Appl Polym Sci 1963, 7, 873.
13. Payne, A. R. J Appl Polym Sci 1962, 6, 57.
14. Payne, A. R. J Appl Polym Sci 1962, 6, 368.
15. Kraus, G. J Appl Polym, Appl Sci Polym Symp 1984, 39, 75.
16. Heinrich, G.; Kluppel, M. Adv Polym Sci 2002, 160, 1.
17. Ulmer, J. D. Rubber Chem Technol 1995, 69, 15.